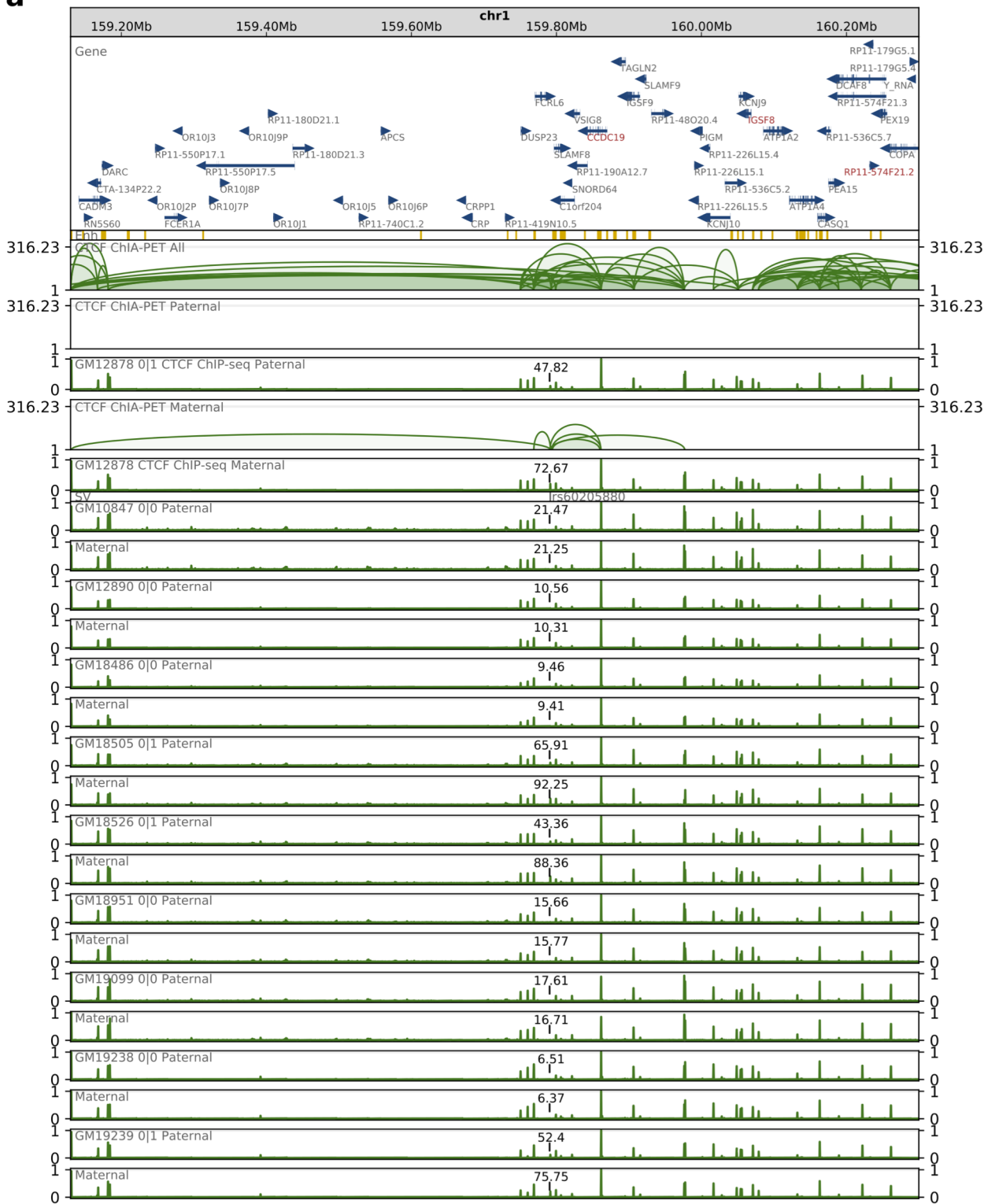
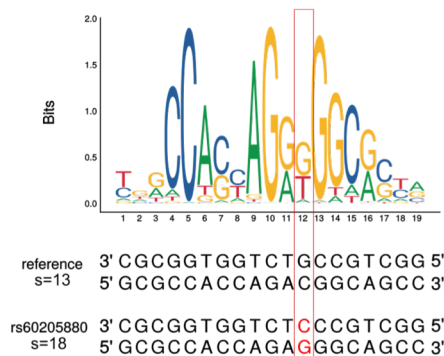


Supplementary Figure 1

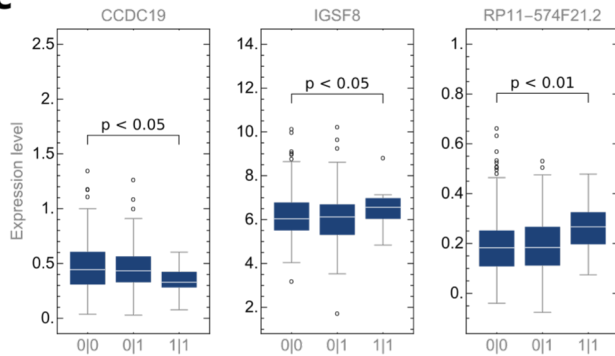
a



b

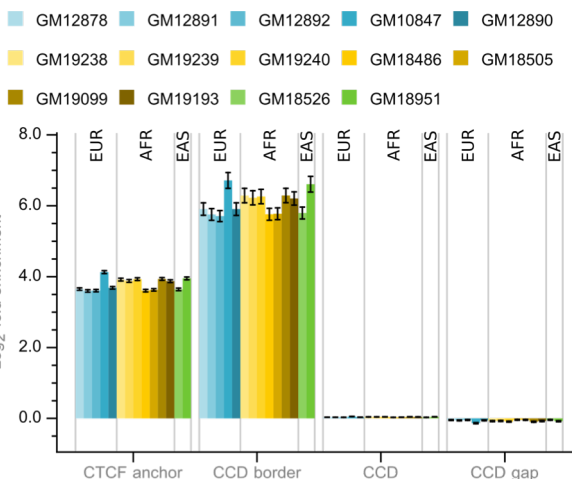


c



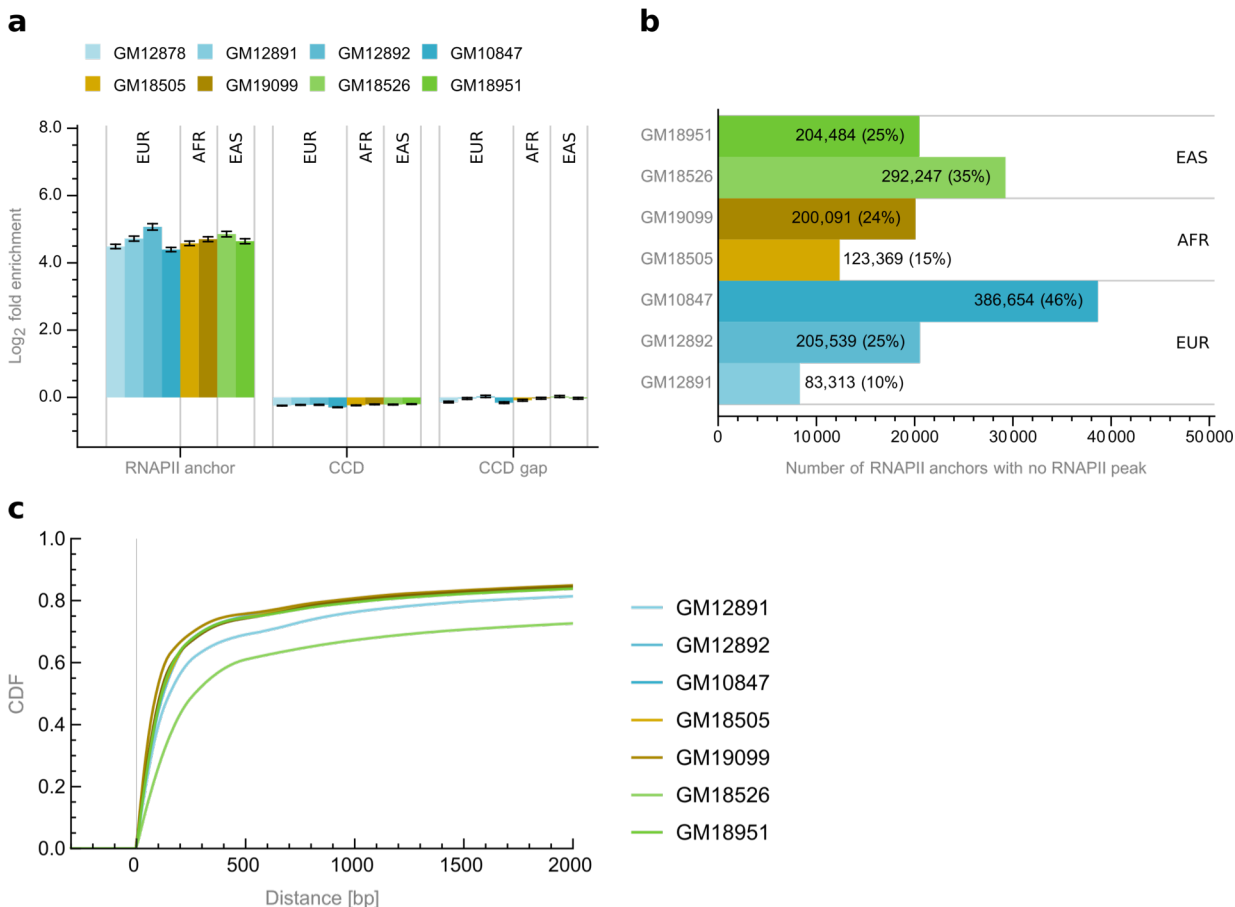
Supplementary Figure 1 SNP in a CTCF motif in region chr1:159130000-160300000. **a**, Browser view of a 1 Mb genomic segment with SNP rs60205880 identified in a part of the human population. SNP rs60205880 alters sequence of a CTCF motif residing in an interaction anchor. Haplotype-specific CTCF ChIP-seq signals from 10 lymphoblastoid cell lines genotyped for this SNP are presented for comparison along with genes, enhancers and haplotype-specific (GM12878) CTCF ChIA-PET interactions located in this genomic segment. ChIP-seq signal from each sample is measured in RPMs and divided by the maximal value of the signal in the visualized region (separately for each homologous chromosome from the pair). In each individual signal track, value of the signal summed over genomic region occupied by the altered CTCF anchor is additionally marked. **b**, Comparison of sequences and scores of CTCF motifs with reference and alternative alleles defined by rs60205880. CTCF sequence logo demonstrates the importance of particular nucleotide positions in the motif. **c**, Differences in gene transcription rates between genotypes set for rs60205880. Only genes exhibiting differences in transcription which pass Mann-Whitney test with p-value < 0.05 were reported.

Supplementary Figure 2



Supplementary Figure 2 Enrichment/depletion of structural elements identified in the GM12878 cell line with CTCF ChIP-seq peaks from different lymphoblastoid cells.

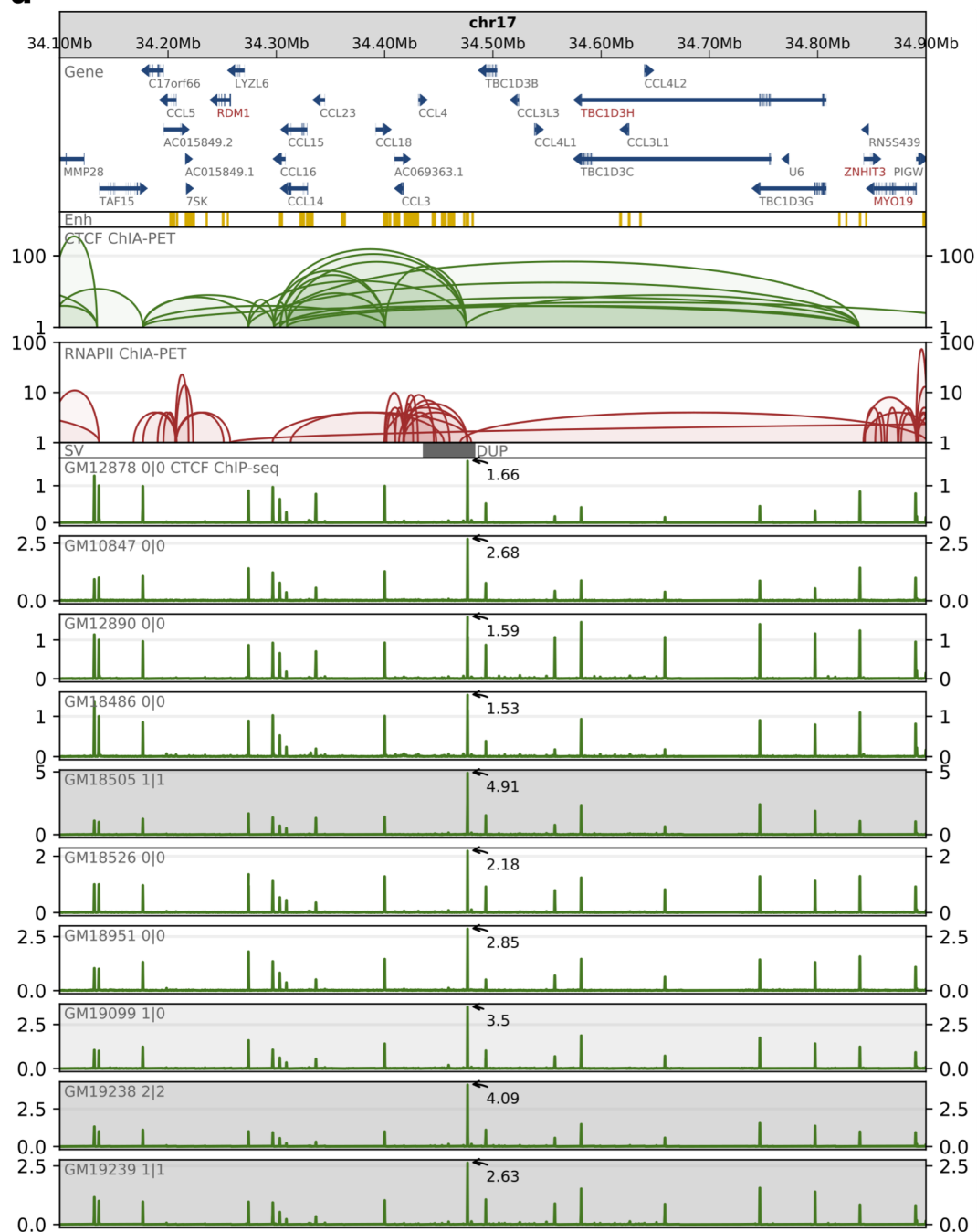
Supplementary Figure 3



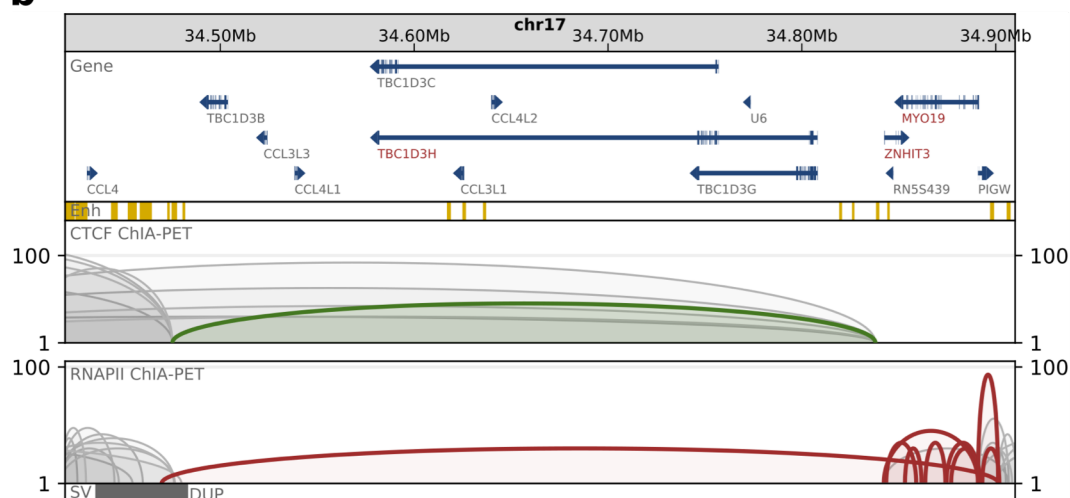
Supplementary Figure 3 RNAPII ChIP-seq peaks in interaction segments. a, Enrichment/depletion of structural elements identified in the GM12878 cell line with RNAPII ChIP-seq peaks from different lymphoblastoid cells. **b,** RNAPII anchors from the GM12878 not intersected with RNAPII ChIP-seq peaks identified in different lymphoblastoid cells. **c,** Cumulative density plot of distances between RNAPII ChIP-seq peaks located in GM12878 interaction anchors and closest RNAPII ChIP-seq peaks from different lymphoblastoid cells.

Supplementary Figure 4

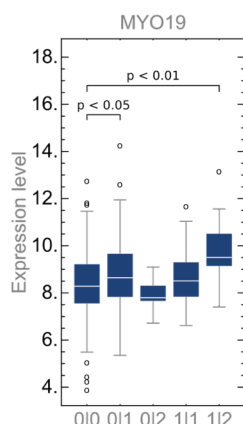
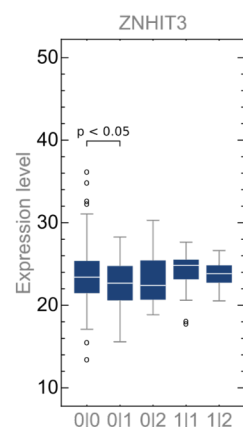
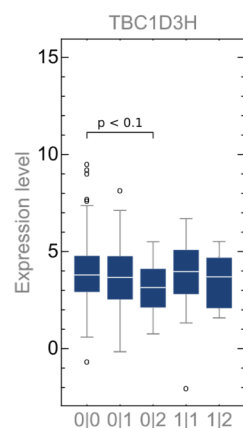
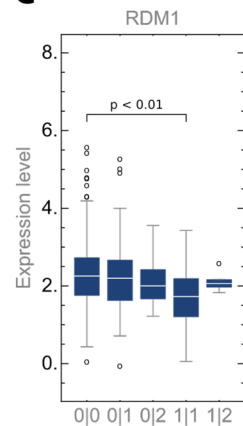
a



b



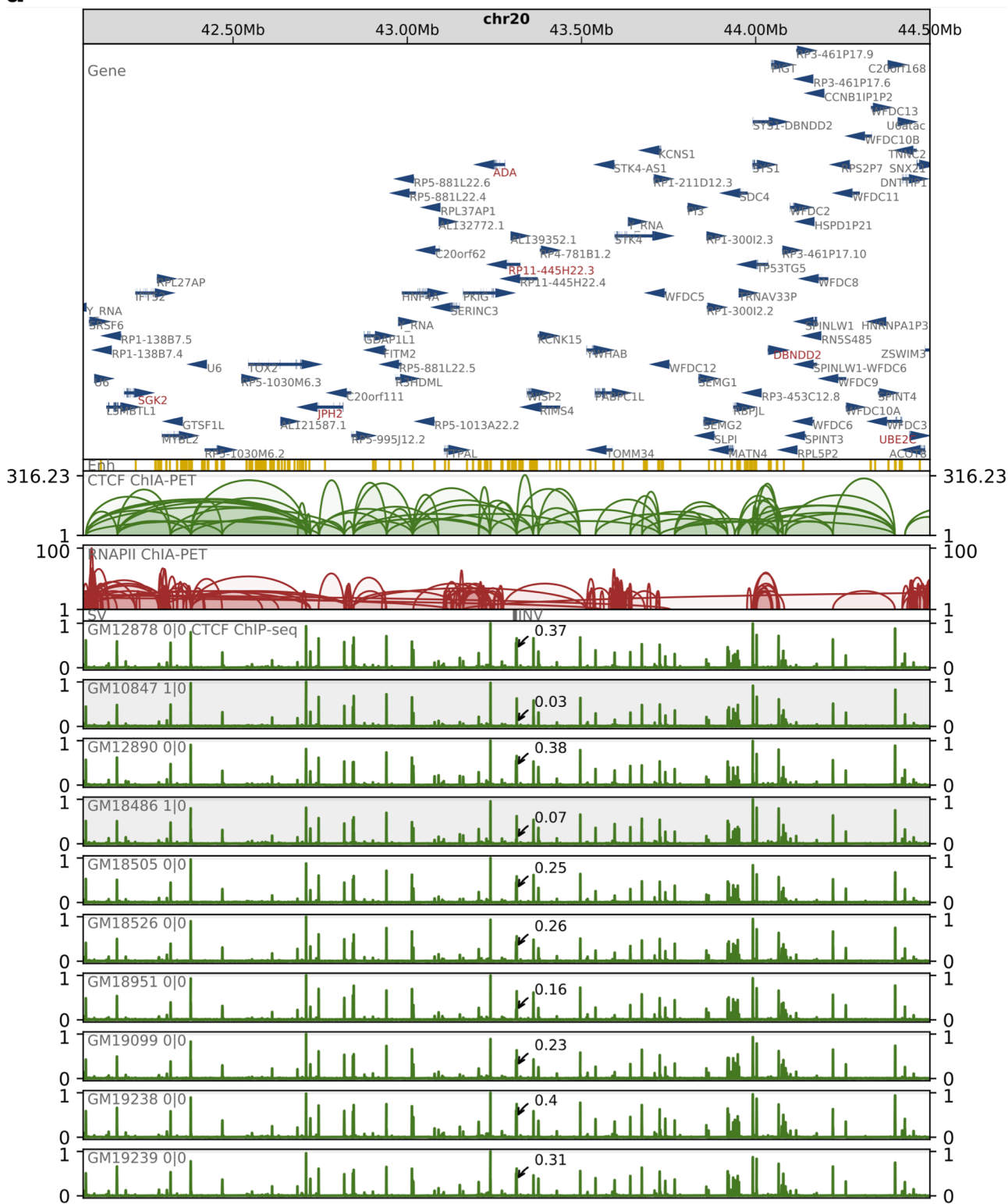
c



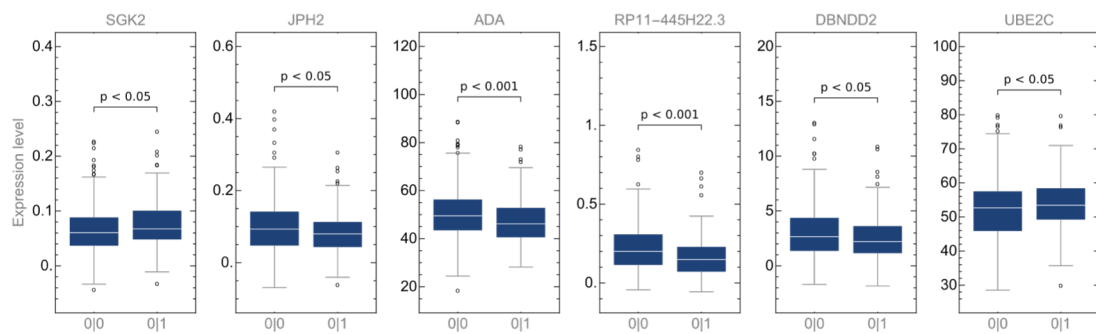
Supplementary Figure 4 Duplication of a CTCF interaction segment in region chr17:34100000-34900000. **a**, Browser view of a 0.8 Mb genomic segment with duplication chr17:34436099-34482872 identified in a part of the human population, which duplicates a CTCF anchor containing enhancers. CTCF ChIP-seq signals from 10 lymphoblastoid cell lines genotyped for this duplication are presented for comparison along with genes, enhancers and CTCF and RNAPII ChIA-PET interactions located in this genomic segment. In each ChIP-seq signal track, the value of the highest signal peak in genomic region targeted by the SV is marked. ChIP-seq signal from each sample is measured in RPMs and divided by the value of the peak neighboring the annotated peak. **b**, Close-up on the CTCF and RNAPII ChIA-PET interactions affected by duplication chr17:34436099-34482872. **c**, Differences in gene transcription rates between genotypes set for duplication chr17:34436099-34482872. Only genes exhibiting differences in transcription which pass Mann-Whitney test with p-value < 0.1 were reported.

Supplementary Figure 5

a



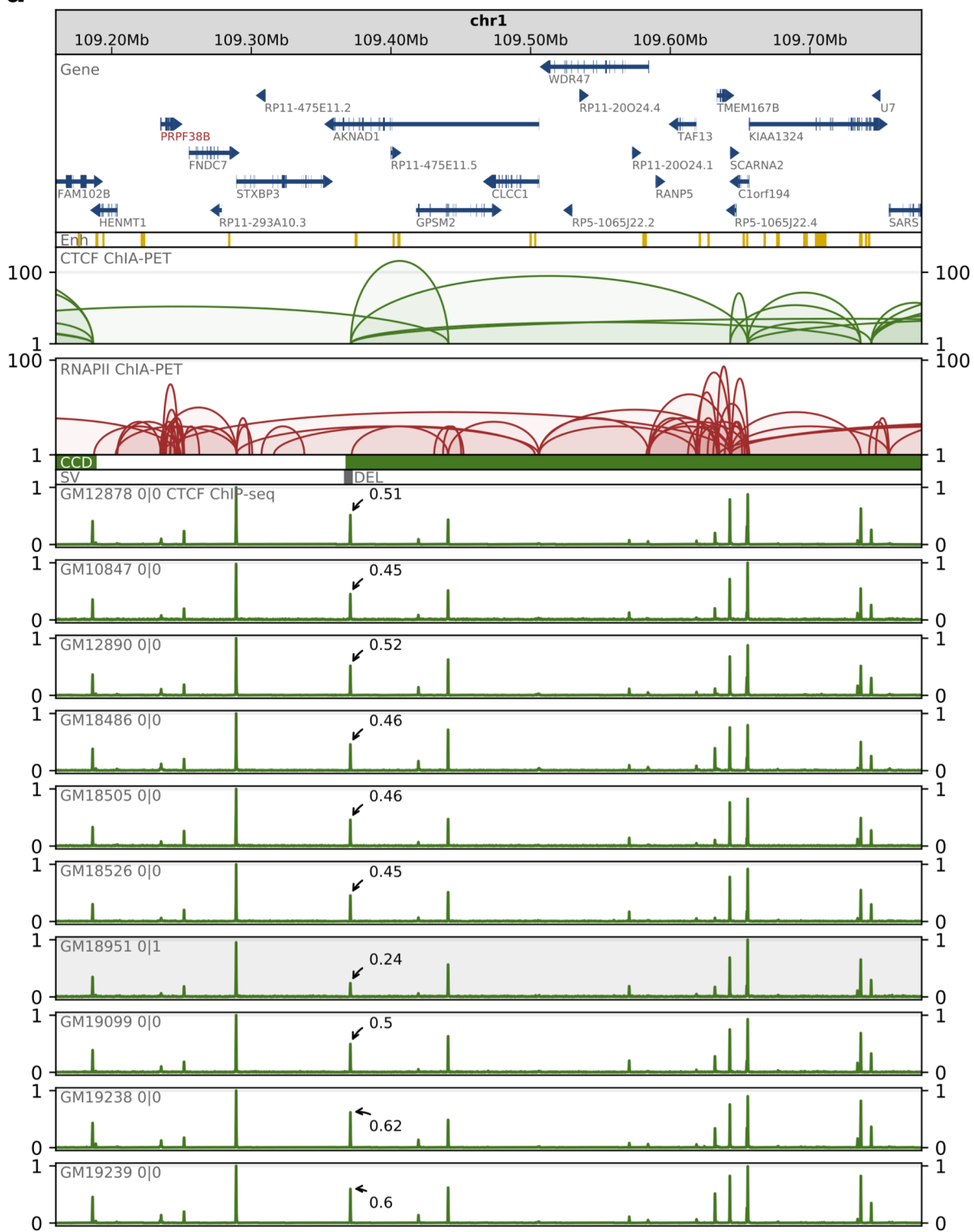
b



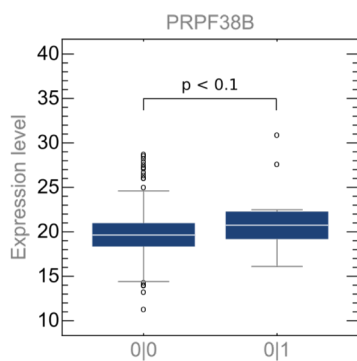
Supplementary Figure 5 Inversion in a CTCF interaction segment in region chr20:42070000-44500000. **a**, Browser view of a 2.5 Mb genomic segment with inversion chr20:43305746-43312261 identified in a part of the human population, which inverts a CTCF motif in an interaction anchor containing an enhancer. CTCF ChIP-seq signals from 10 lymphoblastoid cell lines genotyped for this inversion are presented for comparison along with genes, enhancers and CTCF and RNAPII ChIA-PET interactions located in this genomic segment. ChIP-seq signal from each sample is measured in RPMs and divided by the maximal value of the signal in the visualized region. In each individual signal track, value of the highest signal peak in genomic region targeted by the SV is additionally marked. **b**, Differences in gene transcription rates between genotypes set for inversion chr20:43305746-43312261. Only genes exhibiting differences in transcription which pass Mann-Whitney test with p-value < 0.05 were reported.

Supplementary Figure 6

a



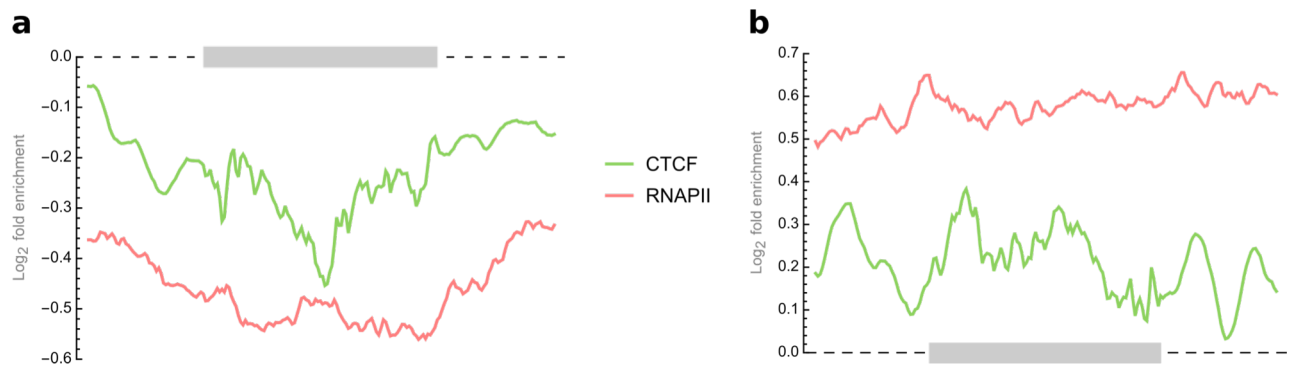
b



Supplementary Figure 6 Deletion of a CCD border in region chr1:109160000-

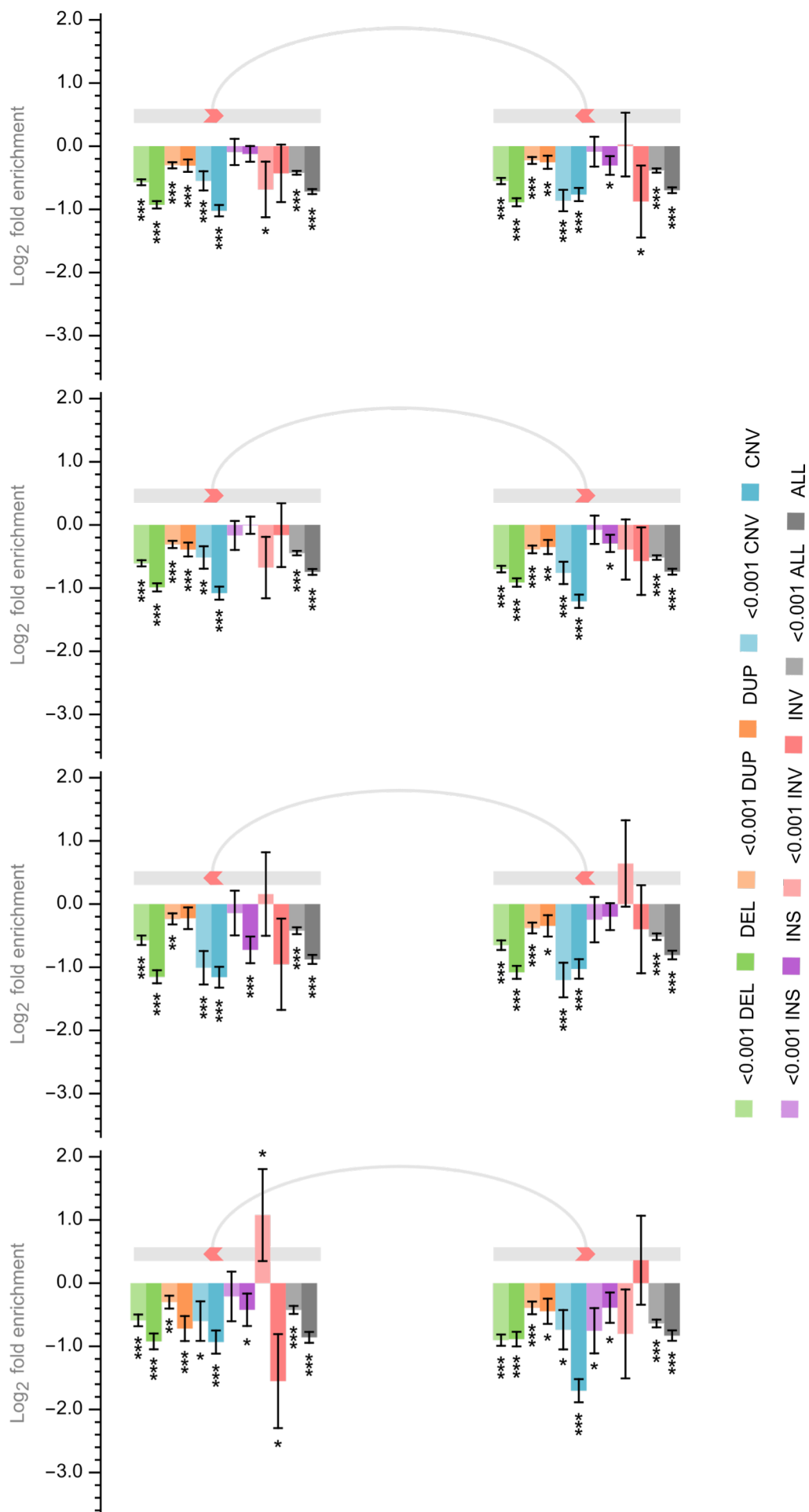
109780000. a, Browser view of a 0.6 Mb genomic segment with deletion chr1:109366972-109372000 identified in a part of the human population, which removes border of a topological domain. CTCF ChIP-seq signals from 10 lymphoblastoid cell lines genotyped for this deletion are presented for comparison along with genes, enhancers and CTCF and RNAPII ChIA-PET interactions located in this genomic segment. ChIP-seq signal from each sample is measured in RPMs and divided by the maximal value of the signal in the visualized region. In each individual signal track, value of the highest signal peak in genomic region targeted by the SV is additionally marked. **b,** Transcription of gene PRPF38B by genotypes set for deletion chr1:109366972-109372000.

Supplementary Figure 7



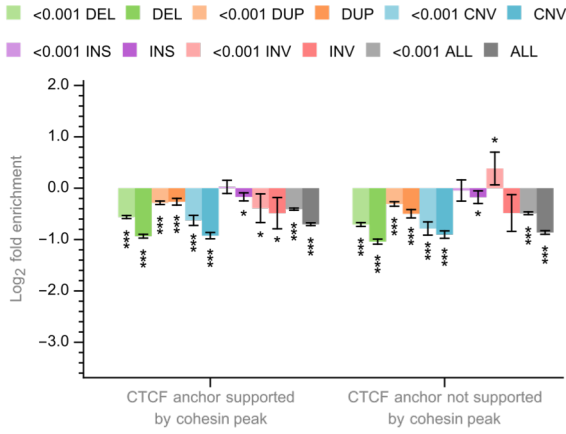
Supplementary Figure 7 Aggregate analysis of ChIP-seq signals in altered interaction anchors. a, Enrichment/depletion of the CTCF and RNAPII ChIP-seq signal in anchors hit by deletions. **b**, Enrichment/depletion of the CTCF and RNAPII ChIP-seq signal in anchors hit by duplications.

Supplementary Figure 8



Supplementary Figure 8 Impact of structural variants on CTCF ChIA-PET interactions in GM12878 cells. Enrichment/depletion of anchors of CTCF PET clusters with SVs of different types and of different VAF (VAF < 0.001 and VAF \geq 0.001). Calculations for convergent, tandem right, tandem left and divergent loops are plotted separately.

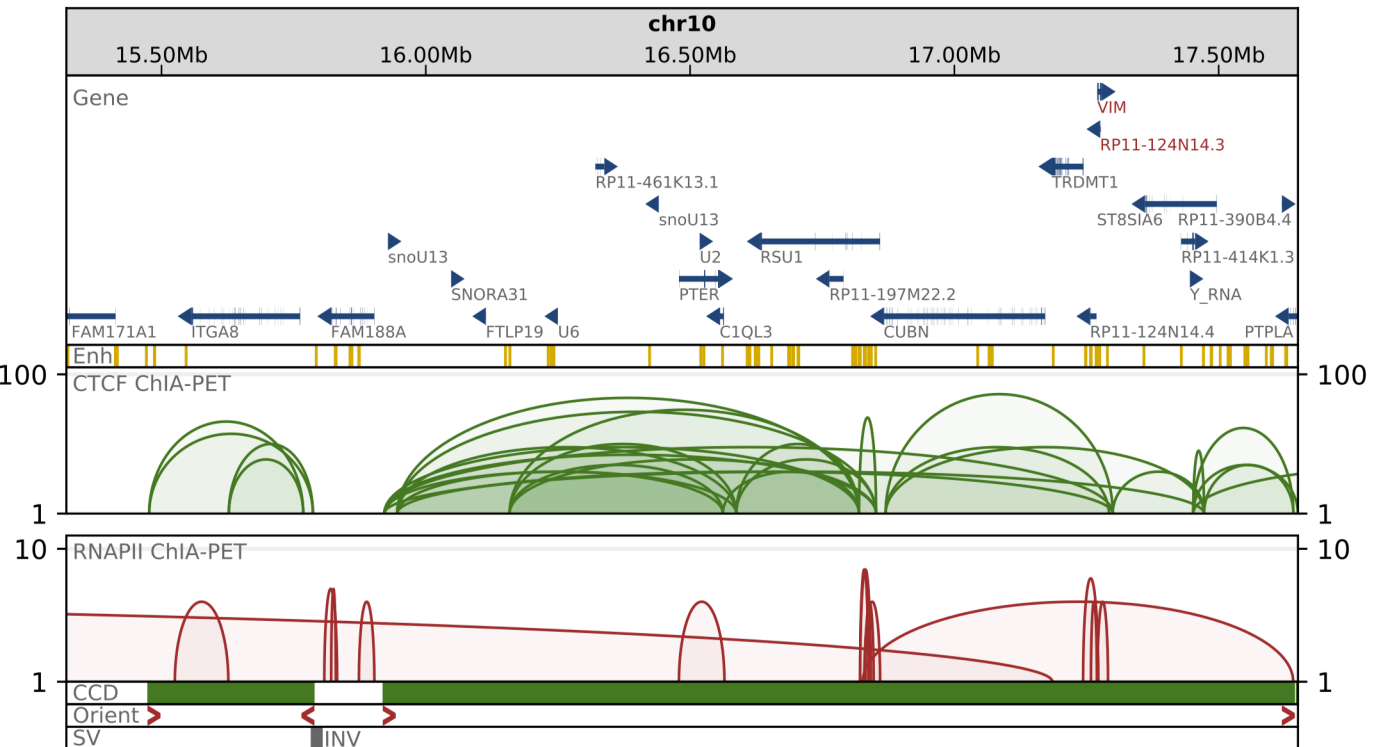
Supplementary Figure 9



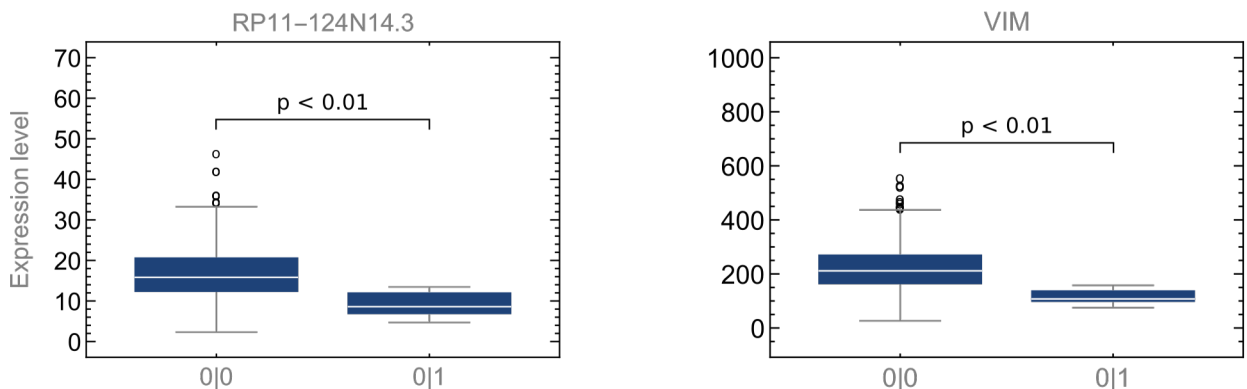
Supplementary Figure 9 Impact of structural variants on CTCF anchors supported by cohesin. Enrichment/depletion of anchors of CTCF PET clusters supported and not supported by cohesin ChIP-seq peaks with SVs of different types and of different VAF (VAF < 0.001 and VAF 0.001).

Supplementary Figure 10

a



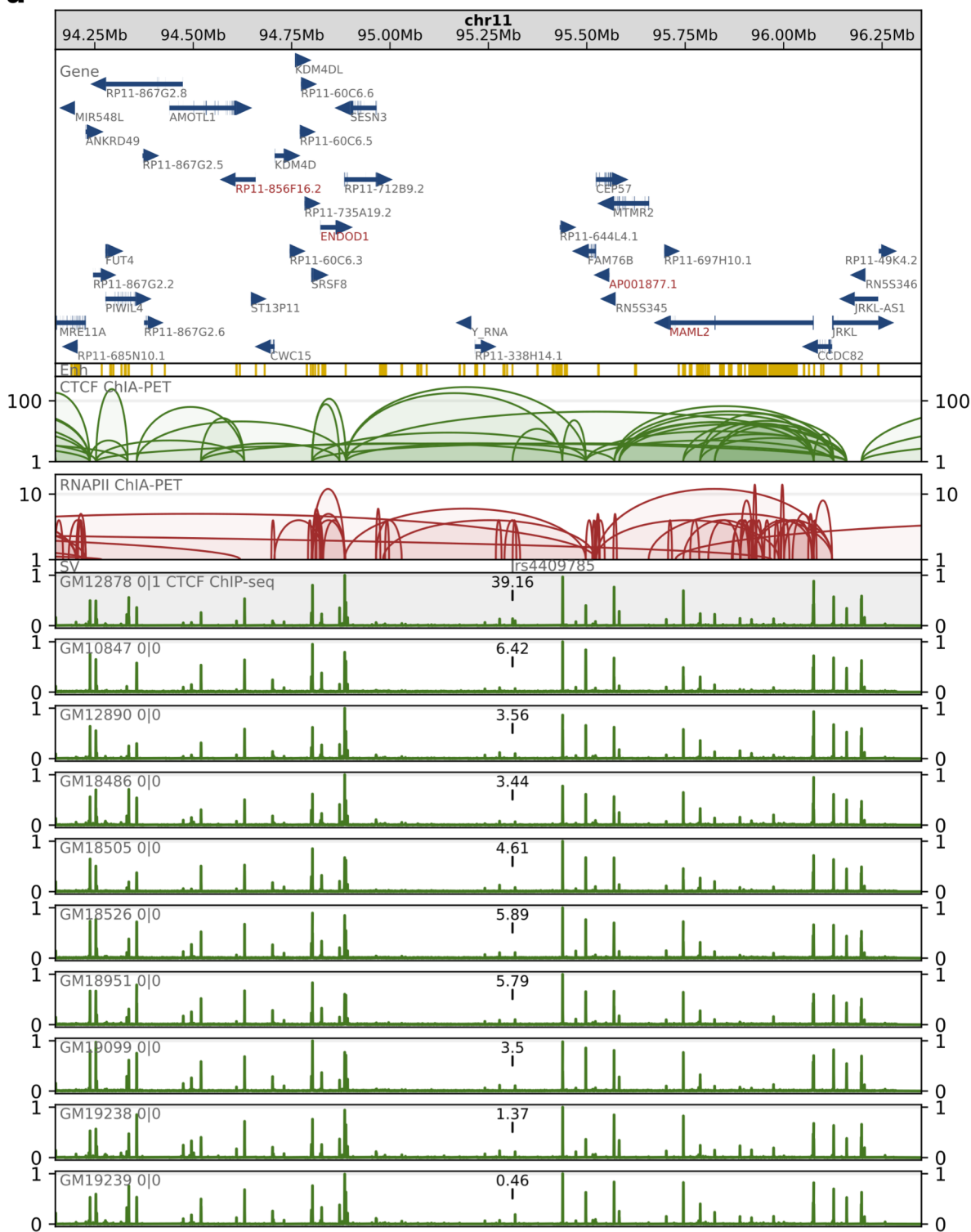
b



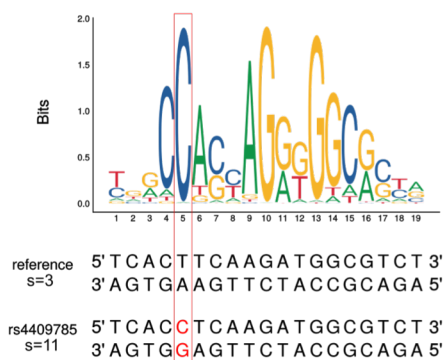
Supplementary Figure 10 Inversion of a CCD border in region chr10:15320000-17650000. **a**, Browser view of a 2 Mb genomic segment with inversion chr10:15784798-15802449 identified in a part of the human population, which inverts a CTCF motif indicating border of a topological domain. Genes, enhancers, orientation of CCD borders, and CTCF and RNAPII ChIA-PET interactions located in this genomic segment are presented. **b**, Differences in gene transcription rates between genotypes set for inversion chr10:15784798-15802449. Only genes exhibiting differences in transcription which pass Mann-Whitney test with p-value < 0.05 were reported.

Supplementary Figure 11

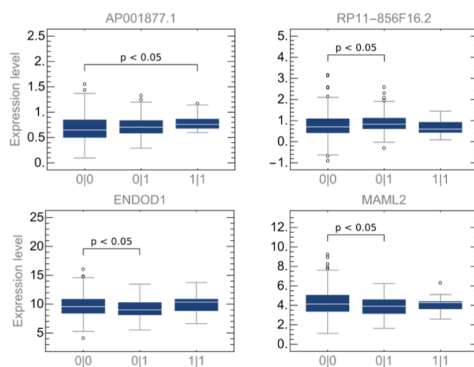
a



b



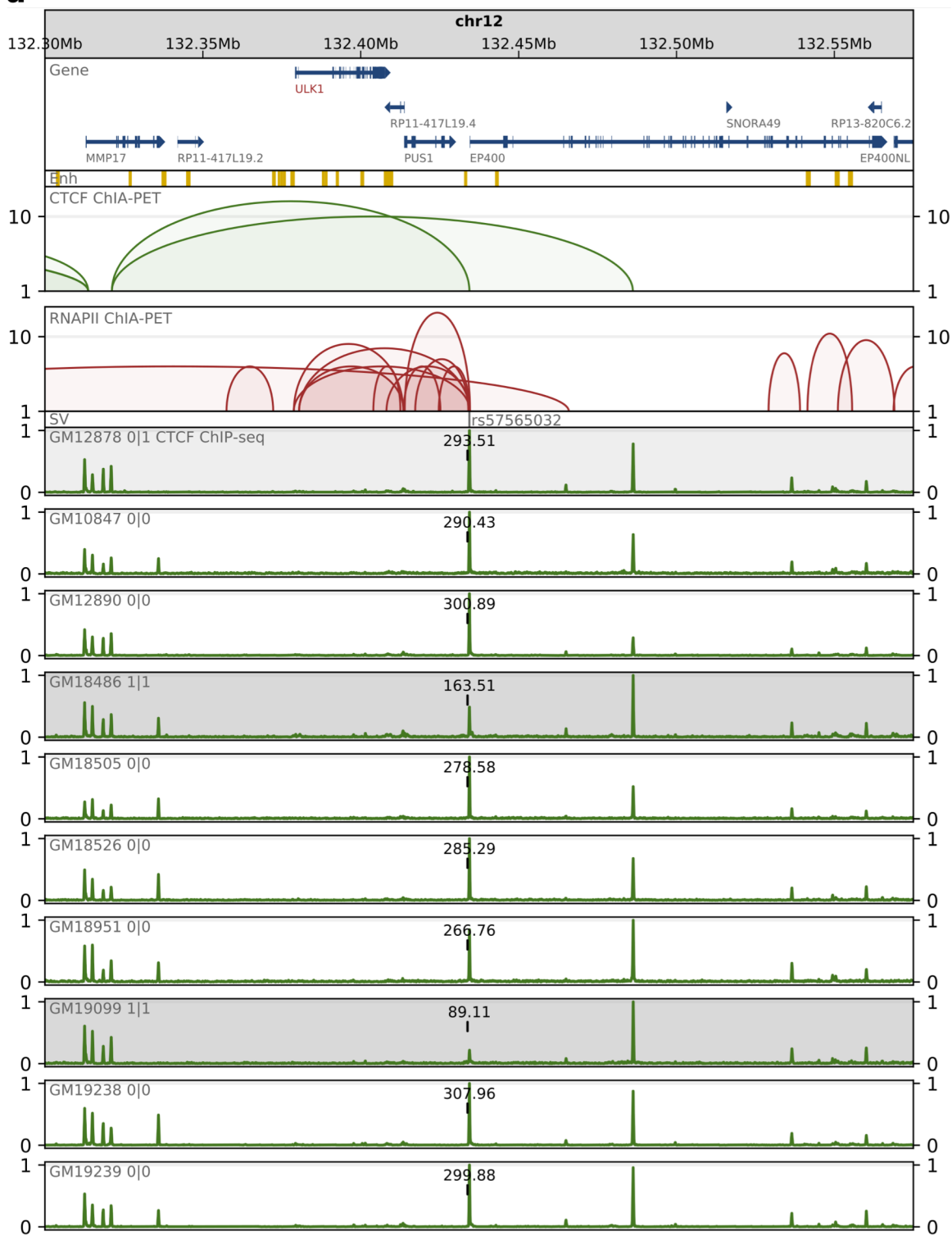
c



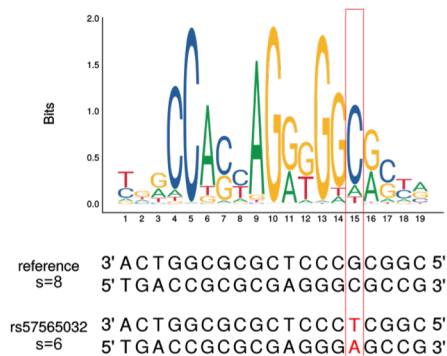
Supplementary Figure 11 GWAS SNP in a CTCF motif in region chr11:94150000-96350000. **a**, Browser view of a 2 Mb genomic segment with SNP rs4409785 identified in a part of the human population and associated with rheumatoid arthritis and vitiligo. SNP rs4409785 alters sequence of a CTCF motif residing in an interaction anchor. CTCF ChIP-seq signals from 10 lymphoblastoid cell lines genotyped for this SNP are presented for comparison along with genes, enhancers and CTCF and RNAPII ChIA-PET interactions located in this genomic segment. ChIP-seq signal from each sample is measured in RPMs and divided by the maximal value of the signal in the visualized region. In each individual signal track, value of the signal summed over genomic region occupied by the altered CTCF anchor is additionally marked. **b**, Comparison of sequences and scores of CTCF motifs with reference and alternative alleles defined by rs4409785. CTCF sequence logo demonstrates the importance of particular nucleotide positions in the motif. **c**, Differences in gene transcription rates between genotypes set for rs4409785. Only genes exhibiting differences in transcription which pass Mann-Whitney test with p-value < 0.05 were reported.

Supplementary Figure 12

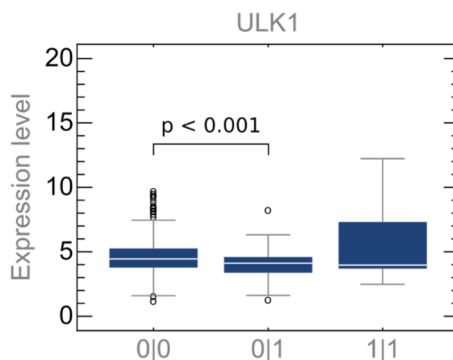
a



b

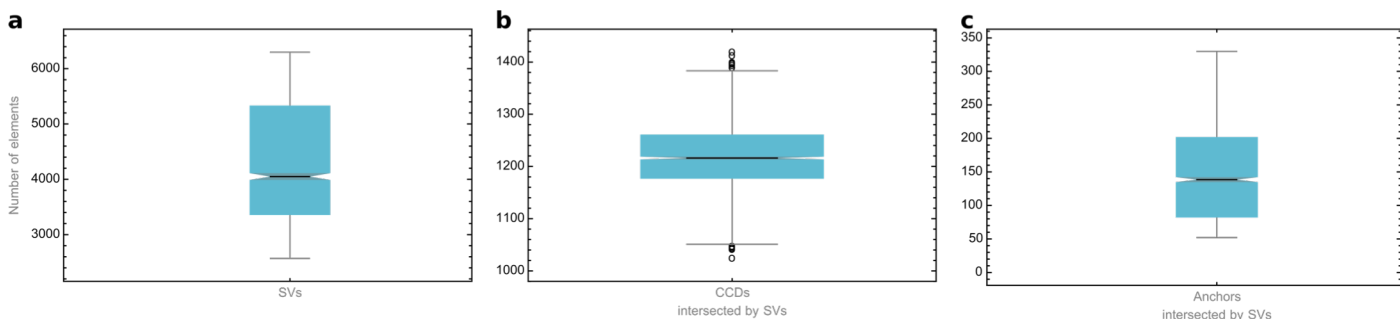


c



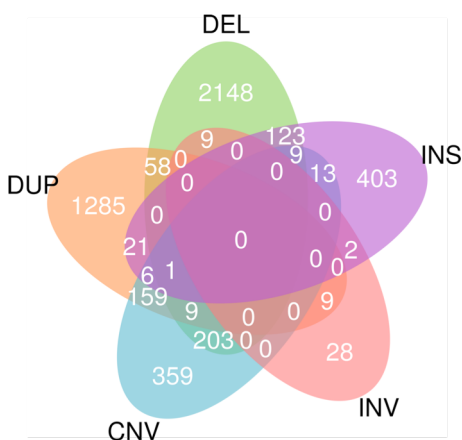
Supplementary Figure 12 GWAS SNP in a CTCF motif in region chr12:132300000-132575000. **a**, Browser view of a 0.3 Mb genomic segment with SNP rs57565032 identified in a part of the human population and associated with red blood cell distribution width. SNP rs57565032 alters sequence of a CTCF motif residing in an interaction anchor. CTCF ChIP-seq signals from 10 lymphoblastoid cell lines genotyped for this SNP are presented for comparison along with genes, enhancers and CTCF and RNAPII ChIA-PET interactions located in this genomic segment. ChIP-seq signal from each sample is measured in RPMs and divided by the maximal value of the signal in the visualized region. In each individual signal track, value of the signal summed over genomic region occupied by the altered CTCF anchor is additionally marked. **b**, Comparison of sequences and scores of CTCF motifs with reference and alternative alleles defined by rs57565032. CTCF sequence logo demonstrates the importance of particular nucleotide positions in the motif. **c**, Transcription of gene ULK1 by genotypes set for rs57565032.

Supplementary Figure 13



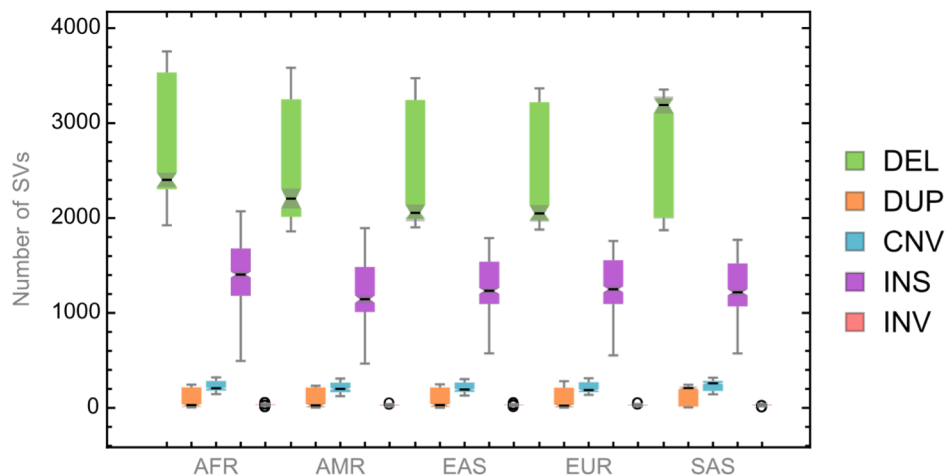
Supplementary Figure 13 Quantification of genomic elements in individual genomes. **a**, Number of SVs (deletions, duplications, inversions and insertions adopted from the 1000 Genomes Project) per sample. **b**, Number of the reference CCDs intersected with SVs in other lymphoblastoid cells. **c**, Number of the reference CTCF anchors intersected with SVs in other lymphoblastoid cells.

Supplementary Figure 14



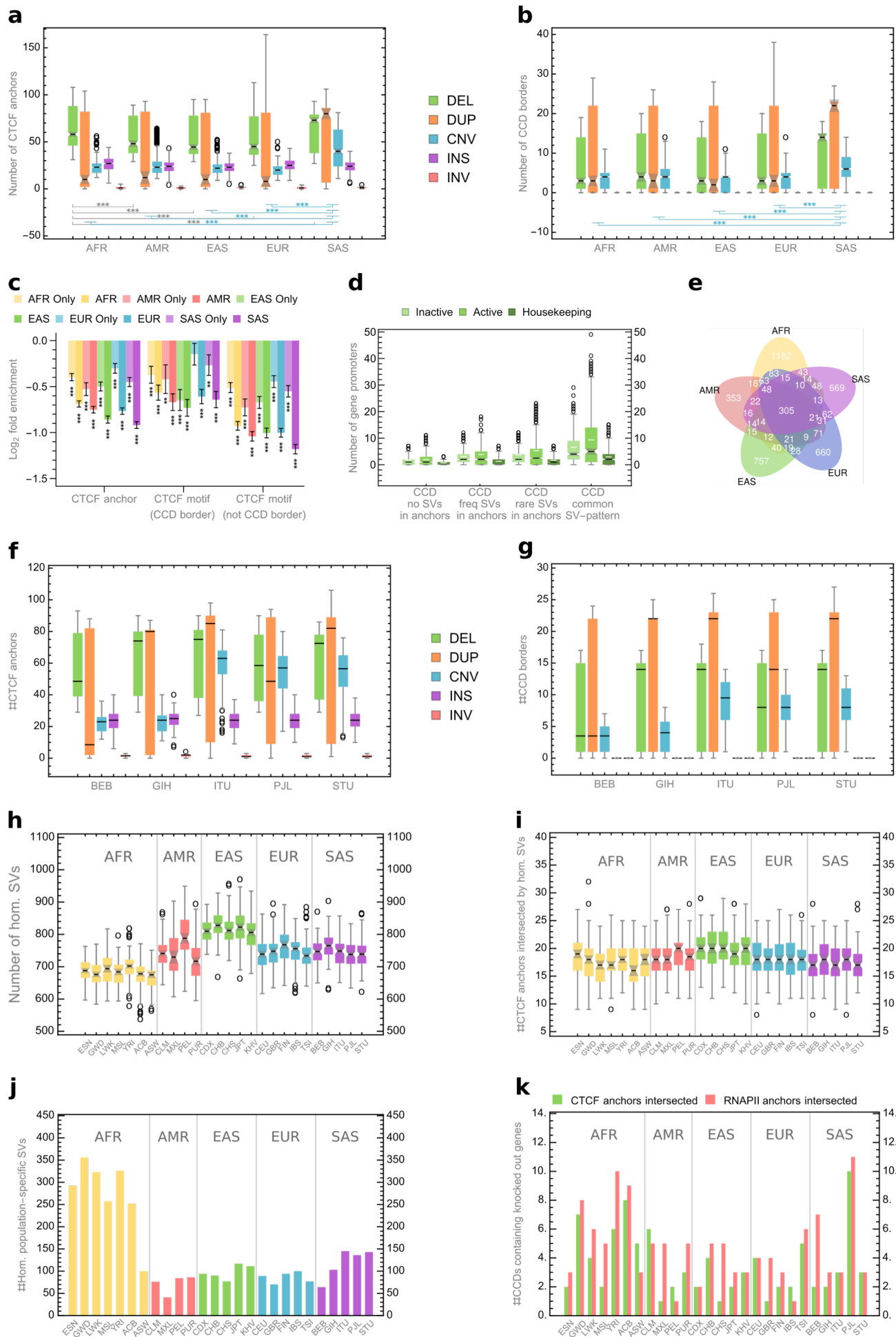
Supplementary Figure 14 Division of domain variability patterns by SV classes they contain.

Supplementary Figure 15



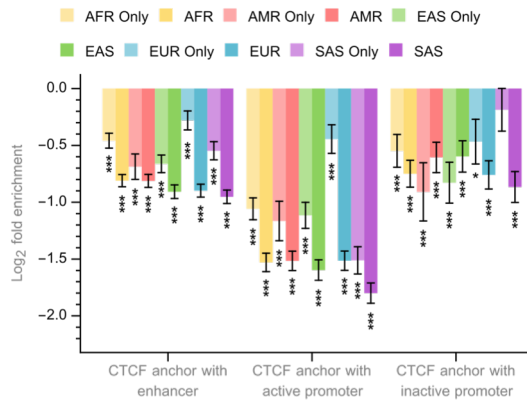
Supplementary Figure 15 Number of SVs per individual genome, grouped by SV class and population.

Supplementary Figure 16



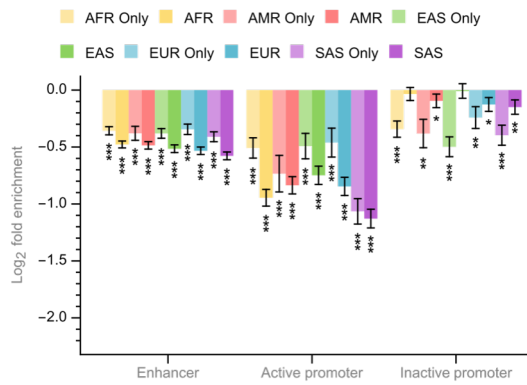
Supplementary Figure 16 Impact of population-specific structural variants on 3D structure of the human genome. **a**, Number of CTCF anchors intersected by SVs of a given type identified in individuals from 5 continental groups. **b**, Number of domain borders fully overlapped by SVs of a given type identified in individuals from 5 continental groups. **c**, Enrichment/depletion of anchors of CTCF PET clusters and borders of CCDs with SVs divided by continental groups. CTCF motifs at CCD borders and outside CCD borders are shown for comparison – only SVs fully covering motifs are counted as hits. **d**, Number of gene promoters in domains covering regions, in which SVs are identified. **e**, Division of domain variability patterns by continental groups they emerge in. **f**, Number of CTCF anchors intersected by SVs of a given type identified in individuals from South Asian continental group. **g**, Number of domain borders fully overlapped by SVs of a given type identified in individuals from South Asian continental group. **h**, Number of homozygous SVs in individual human genomes divided by population. CNVs are treated as homozygous when number of copies on both homologous chromosomes is different than in the reference (hom. – homozygous). **i**, Number of CTCF anchors intersected by homozygous SVs in individual genomes divided by population. **j**, Homozygous SVs identified in only one human population. **k**, Number of CCDs containing human knockouts with CTCF (green) or RNAPII (red) anchors intersected by homozygous population-specific SVs.

Supplementary Figure 17



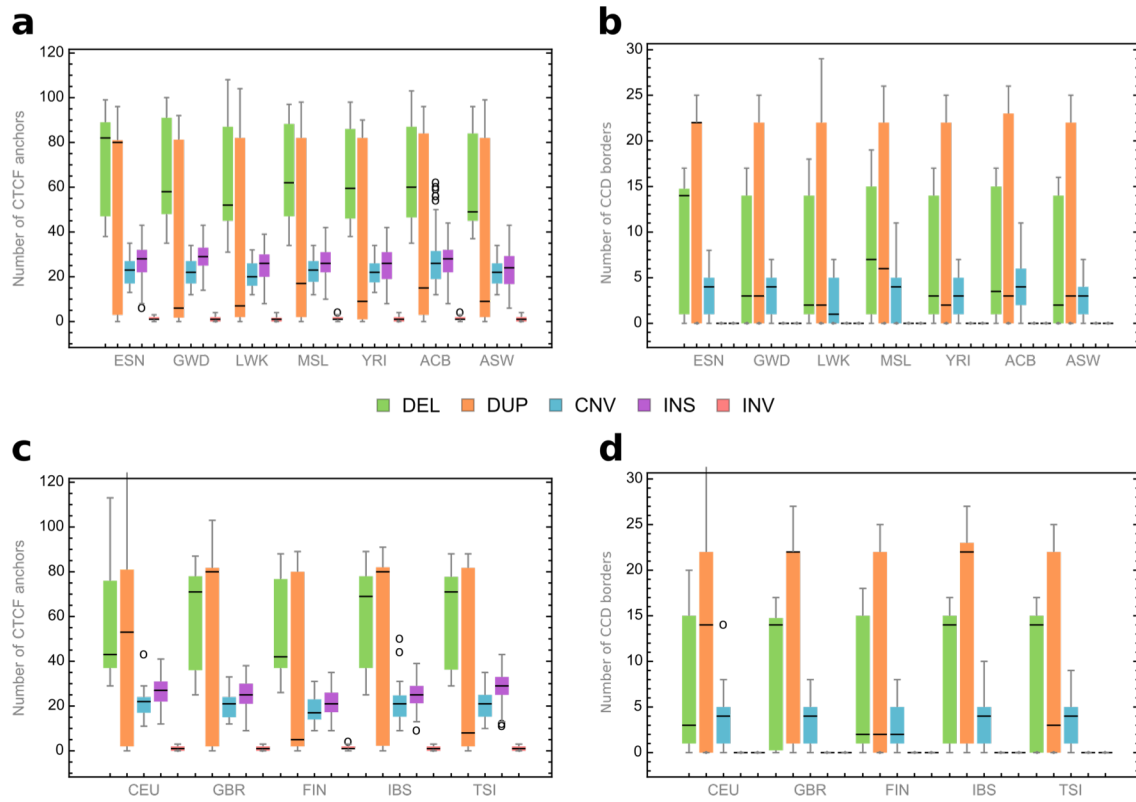
Supplementary Figure 17 Enrichment/depletion of CTCF anchors intersected with genomic functional elements identified in GM12878 cells with SVs divided by continental groups.

Supplementary Figure 18



Supplementary Figure 18 Enrichment/depletion of genomic functional elements identified in GM12878 cells with SVs divided by continental groups.

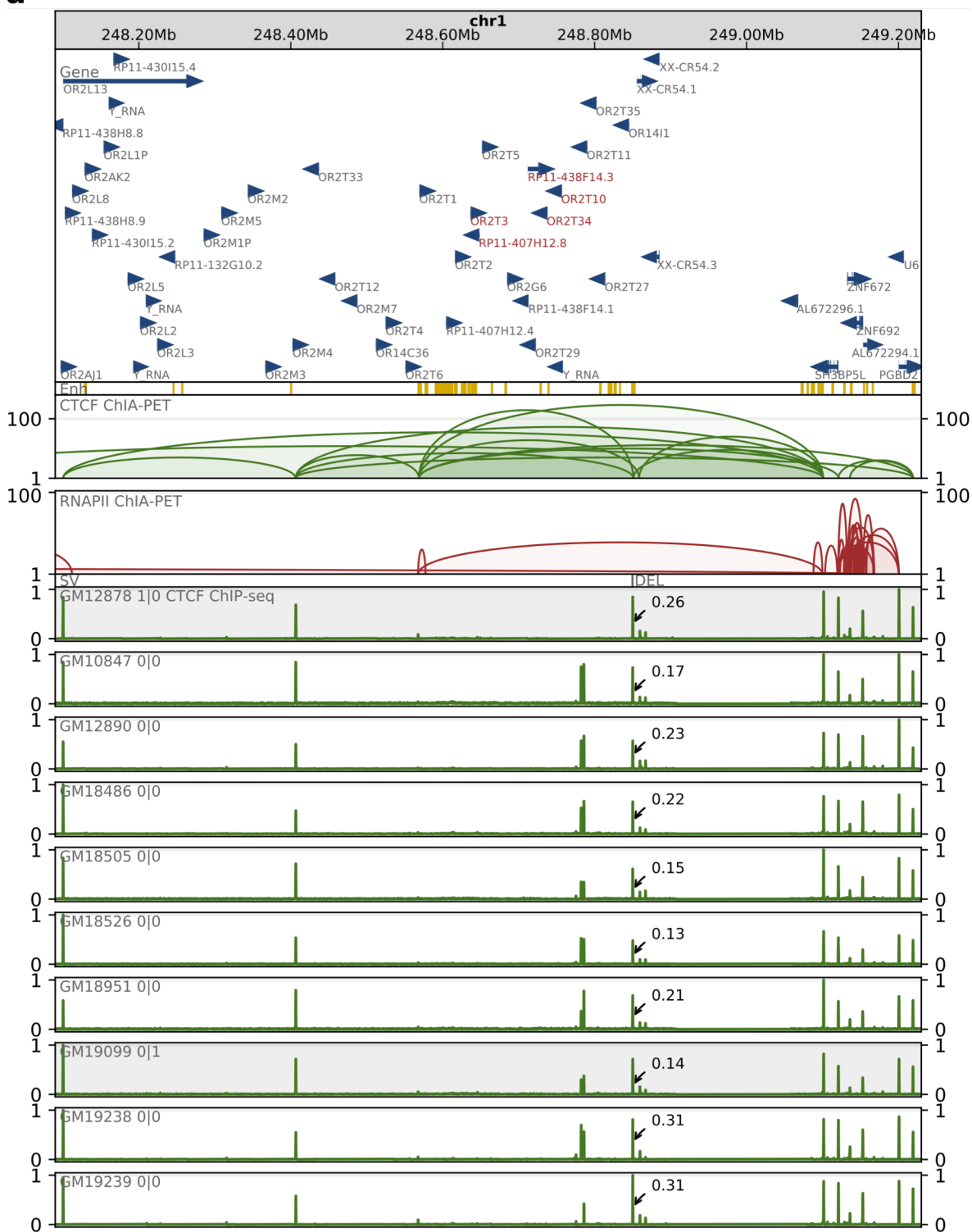
Supplementary Figure 19



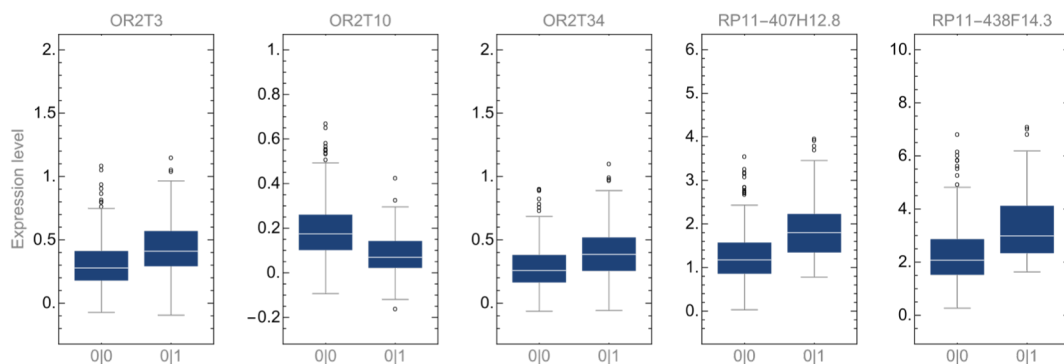
Supplementary Figure 19 Individual structural variation in African and European continental groups. a, Number of CTCF anchors intersected by SVs of a given type identified in individuals from African continental group. **b,** Number of domain borders fully overlapped by SVs of a given type identified in individuals from African continental group. **c,** Similar to (a), but for European continental group. **d,** Similar to (b), but for European continental group.

Supplementary Figure 20

a



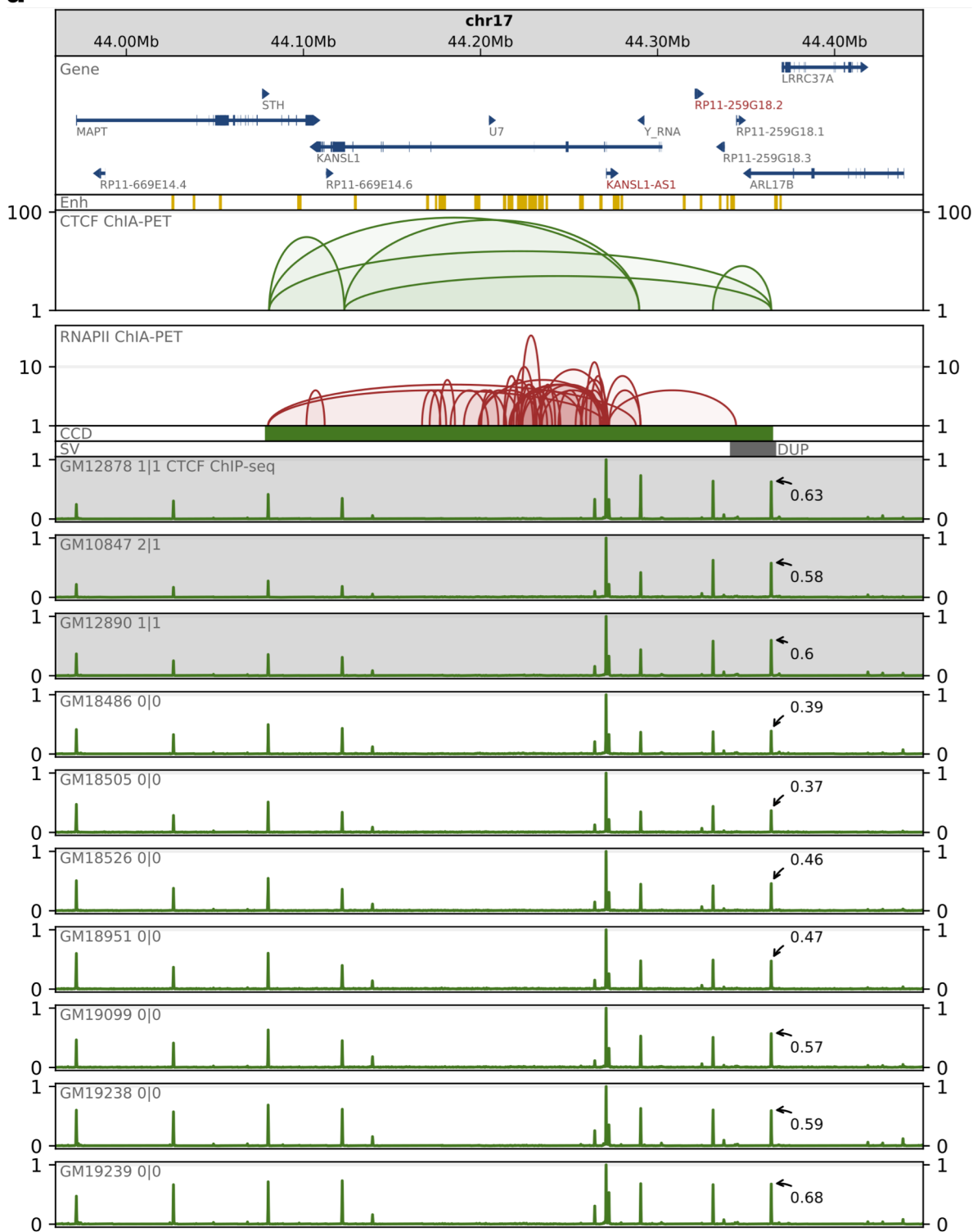
b



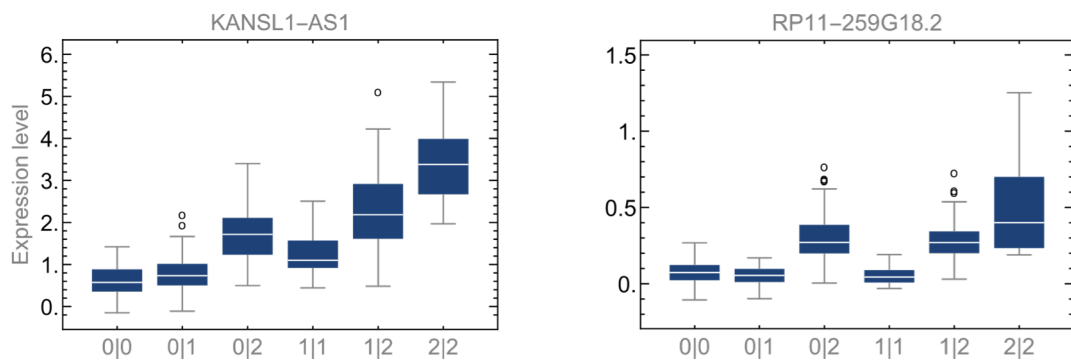
Supplementary Figure 20 Deletion in a CTCF interaction segment in region chr1:248090000-249230000. **a**, Browser view of a 1 Mb genomic segment with deletion chr1:248849861-248850138 identified in a part of the human population, which excises the strongest CTCF motif in an interaction anchor and is an eQTL for 5 neighboring genes (signed with the red font). CTCF ChIP-seq signals from 10 lymphoblastoid cell lines genotyped for this deletion are presented for comparison along with genes, enhancers and CTCF and RNAPII ChIA-PET interactions located in this genomic segment. ChIP-seq signal from each sample is measured in RPMs and divided by the maximal value of the signal in the visualized region. In each individual signal track, value of the highest signal peak in genomic region targeted by the SV is additionally marked. **b**, Genes which transcription is correlated with deletion chr1:248849861-248850138 (p-value much smaller than 0.001).

Supplementary Figure 21

a

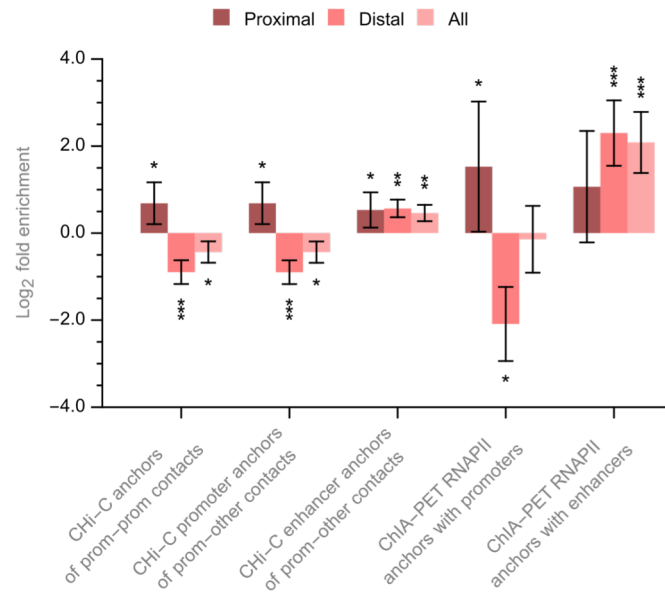


b



Supplementary Figure 21 Duplication of a CCD border in region chr17:43960000-44450000. **a**, Browser view of a 0.5 Mb genomic segment with duplication chr17:44341412-44366497 identified in a part of the human population, which duplicates border of a topological domain and is an eQTL for 2 neighboring genes (signed with the red font). CTCF ChIP-seq signals from 10 lymphoblastoid cell lines genotyped for this duplication are presented for comparison along with genes, enhancers and CTCF and RNAPII ChIA-PET interactions located in this genomic segment. ChIP-seq signal from each sample is measured in RPMs and divided by the maximal value of the signal in the visualized region. In each individual signal track, value of the highest signal peak in genomic region targeted by the SV is additionally marked. **b**, Genes which transcription is correlated with duplication chr17:44341412-44366497 (p-value much smaller than 0.001).

Supplementary Figure 22

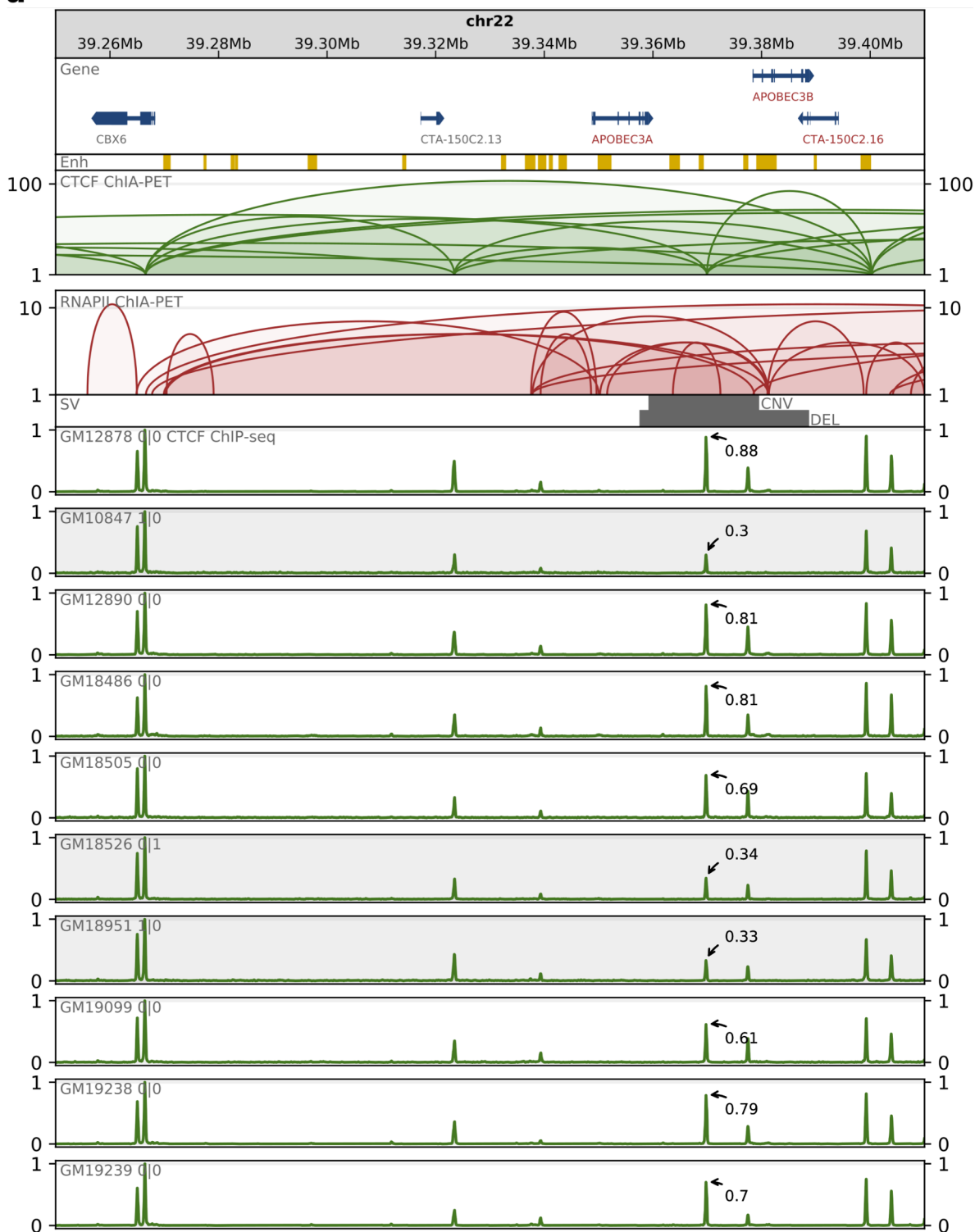


Supplementary Figure 22 eQTLs versus promoter interactions.

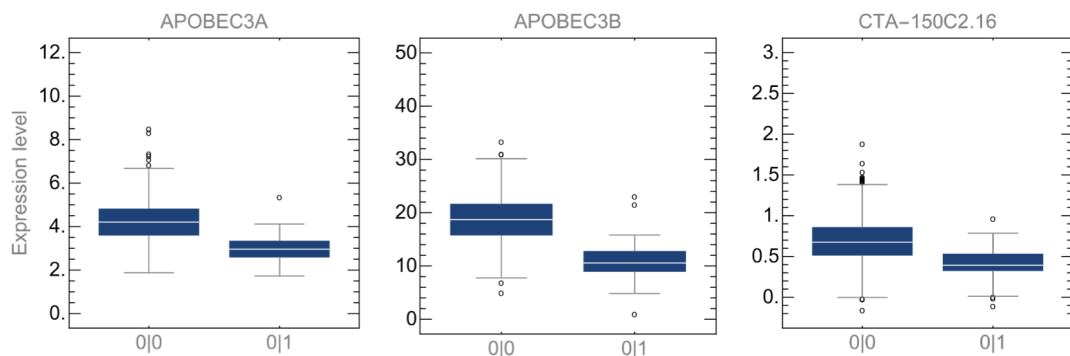
Enrichment/depletion of ChIA-PET and ChI-C anchors containing promoters or enhancers with proximal and distal eQTLs. ChI-C anchors were divided into 3 groups: anchors of promoter-promoter interactions, promoter anchors of promoter-other region interactions and anchors intersected by enhancers of promoter-other region interactions.

Supplementary Figure 23

a



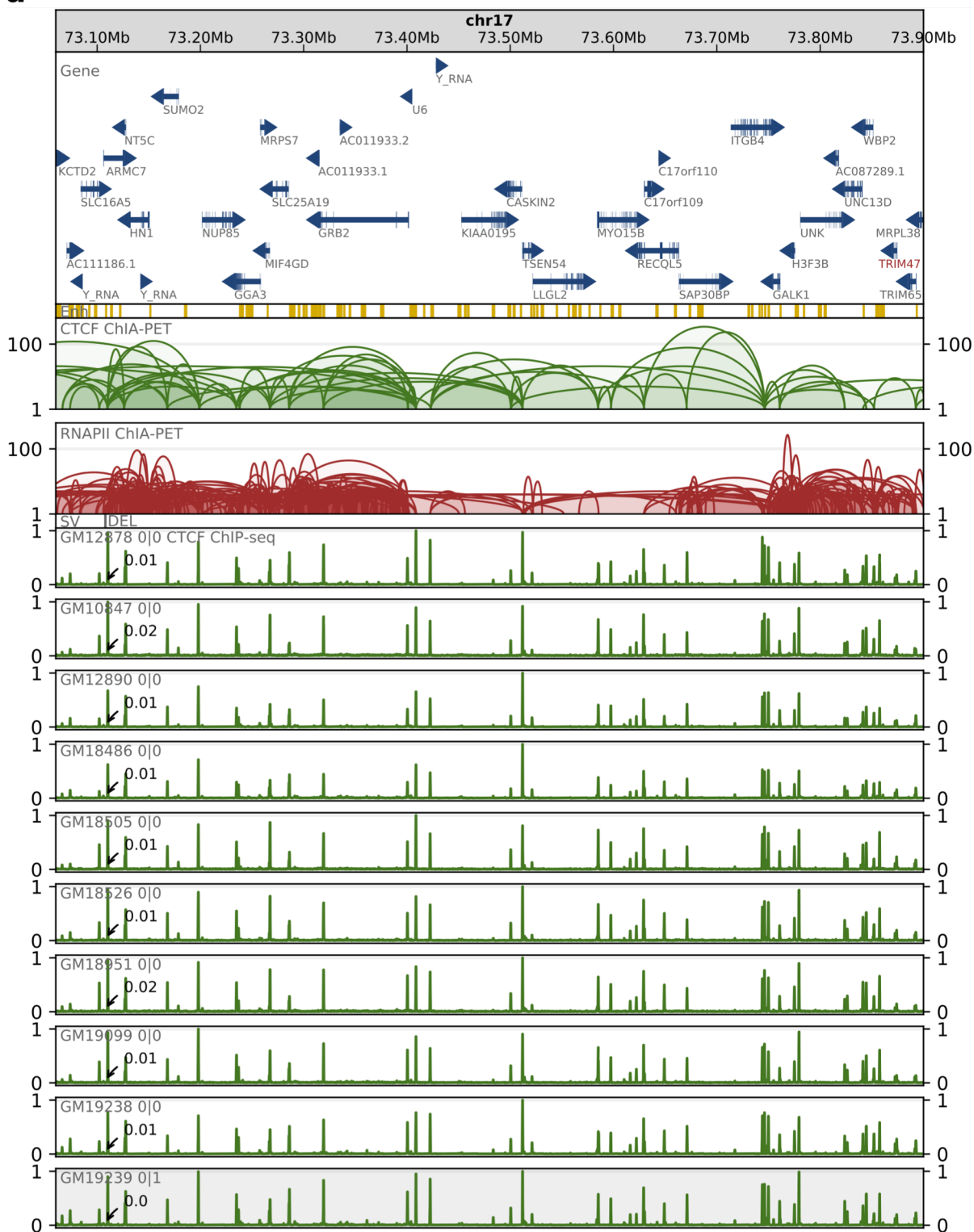
b



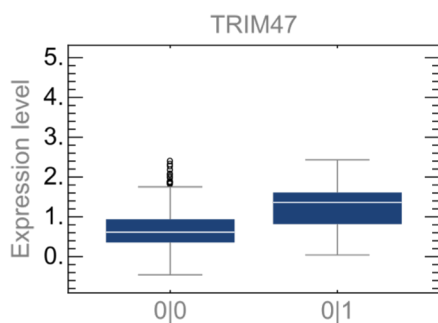
Supplementary Figure 23 Deletion of a CTCF interaction segment in region chr22:39250000-39410000. **a**, Browser view of a 0.2 Mb genomic segment with deletion chr22:39357694-39388574/CNV chr22:39359355-39379392 identified in a part of the human population, which removes/removes or multiplies CTCF anchor and is an eQTL for 3 neighboring genes (signed with the red font). APOBEC3A and APOBEC3B are immune-related genes. CTCF ChIP-seq signals from 10 lymphoblastoid cell lines are presented for comparison along with genes, enhancers and CTCF and RNAPII ChIA-PET interactions located in this genomic segment. All the presented cell lines with non-reference genotypes carry deletion chr22:39357694-39388574. ChIP-seq signal from each sample is measured in RPMs and divided by the maximal value of the signal in the visualized region. In each individual signal track, value of the highest signal peak in genomic region targeted by the SV is additionally marked. **b**, Genes which transcription is correlated with deletion chr22:39357694-39388574 and CNV chr22:39359355-39379392 (p-value much smaller than 0.001).

Supplementary Figure 24

a

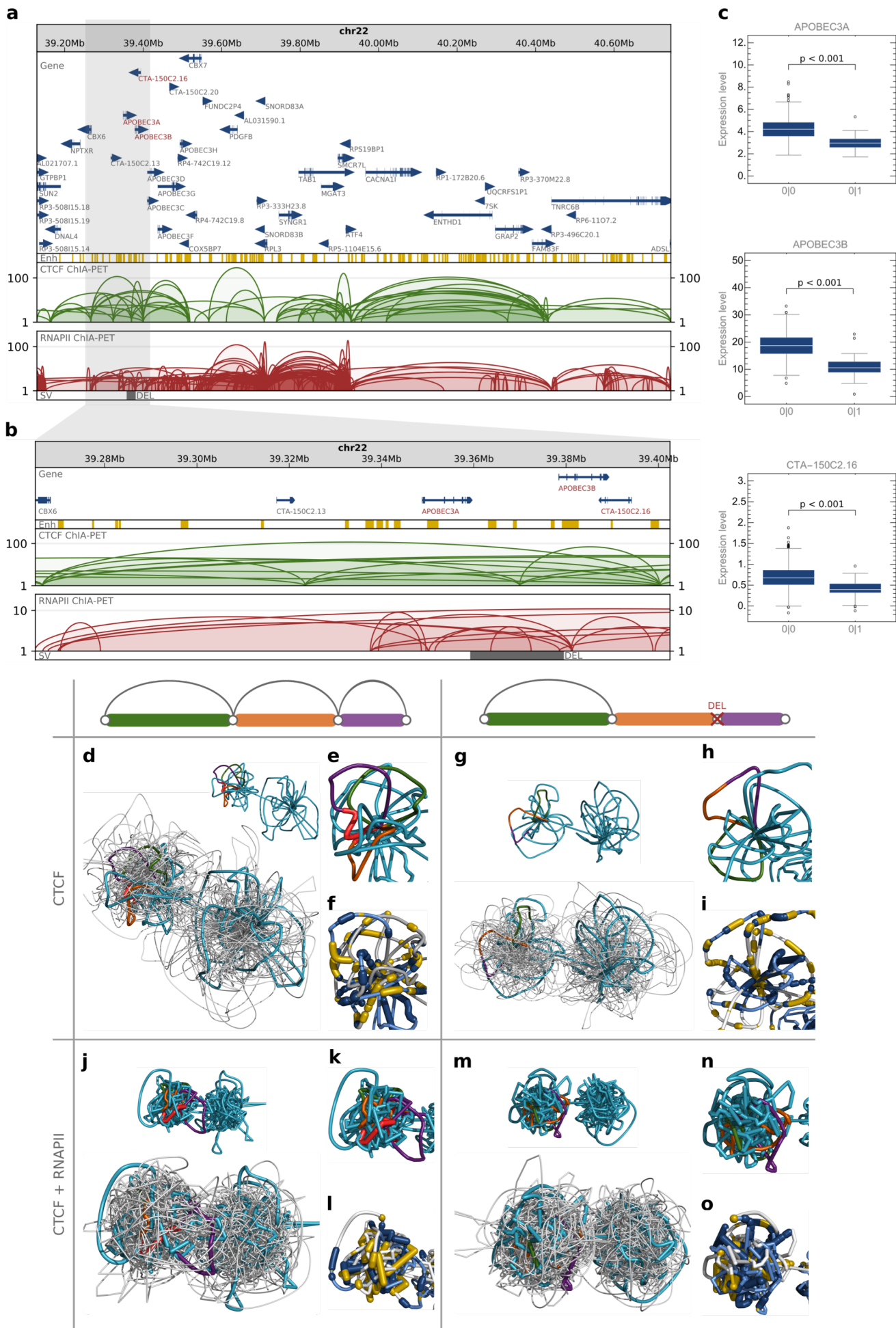


b



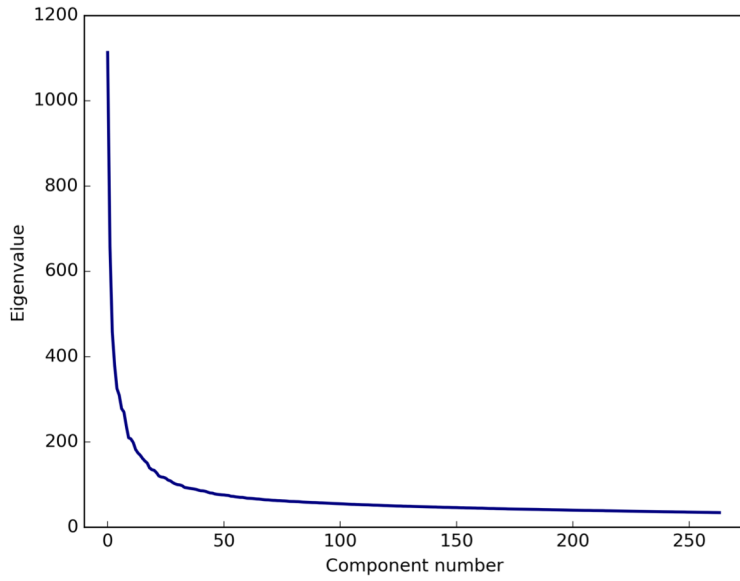
Supplementary Figure 24 Deletion in a CTCF interaction segment in region chr17:73060000-73900000. **a**, Browser view of a 0.8 Mb genomic segment with deletion chr17:73107713-73108273 identified in a part of the human population, which removes part of a CTCF anchor and is an eQTL for immune-related gene TRIM47 (signed with the red font). CTCF ChIP-seq signals from 10 lymphoblastoid cell lines genotyped for this deletion are presented for comparison along with genes, enhancers and CTCF and RNAPII ChIA-PET interactions located in this genomic segment. ChIP-seq signal from each sample is measured in RPMs and divided by the maximal value of the signal in the visualized region. In each individual signal track, value of the highest signal peak in genomic region targeted by the SV is additionally marked. **b**, Immune-related gene TRIM47 which transcription is correlated with deletion chr17:73107713-73108273 (p-value much smaller than 0.001).

Supplementary Figure 25



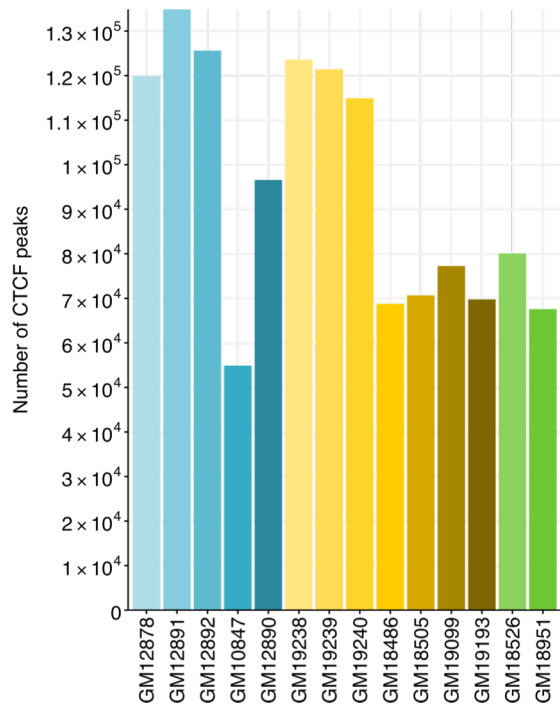
Supplementary Figure 25 Computational models of chromatin structures impacted by SV. **a**, Browser view of a 1.6 Mb topological domain (chr22:39129240-40744672) with deletion chr22:39359355-39379392 identified in a part of the human population, which removes CTCF anchor and is an eQTL for 3 neighboring genes (signed with the red font). APOBEC3A and APOBEC3B are immune-related genes. Genes, enhancers and CTCF and RNAPII ChIA-PET interactions located in this genomic segment are presented. **b**, Close-up on the CTCF and RNAPII ChIA-PET interactions affected by deletion chr22:39359355-39379392. **c**, Genes which transcription is correlated with deletion chr22:39359355-39379392 (p-value much smaller than 0.001). **d**, Ensemble of 10 3D models of domain chr22:39129240-40744672 based on CTCF ChIA-PET data. A centroid structure is cyan and has chromatin loops shown in (b) colored as in the schematic drawing. All other structures in ensemble are gray. The centroid structure is also presented alone. **e**, Close-up on the chromatin loops forming region shown in (b). **f**, Similar to (d), but genes and enhancers are marked. **g - i**, Similar to (d - f), but structures with deletion chr22:39359355-39379392 are modeled. **j - l**, Similar to (g - i), but here both CTCF and RNAPII ChIA-PET contacts were used to reconstruct the 3D structures. **m - o**, Similar to (j - l), but structures with deletion chr22:39359355-39379392 are modeled.

Supplementary Figure 26



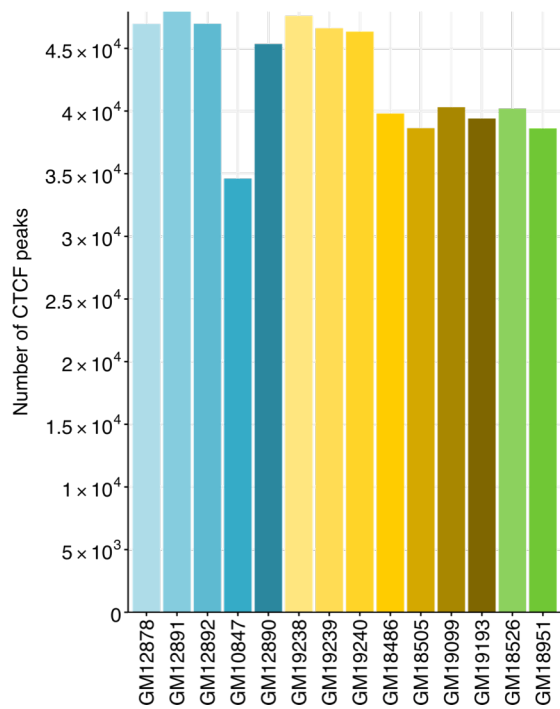
Supplementary Figure 26 Scree Plot. Showing sorted eigenvalues for PCA applied to the space of gene expression rates.

Supplementary Figure 27



Supplementary Figure 27 Number of CTCF ChIP-seq peaks called in different human lymphoblastoid cell lines.

Supplementary Figure 28



Supplementary Figure 28 Number of CTCF ChIP-seq peaks called in different human lymphoblastoid cell lines after filtering by conserved CTCF binding sites.

Supplementary Table 1

Population		Code
African ancestry (AFR)		
Esan in Nigeria	Esan	ESN
Gambian in Western Division, Mandinka	Gambian	GWD
Luhya in Webuye, Kenya	Luhya	LWK
Mende in Sierra Leone	Mende	MSL
Yoruba in Ibadan, Nigeria	Yoruba	YRI
African Caribbean in Barbados	Barbadian	ACB
People with African Ancestry in Southwest USA	African-American SW	ASW
Americas (AMR)		
Colombians in Medellin, Colombia	Colombian	CLM
People with Mexican Ancestry in Los Angeles, CA, USA	Mexican-American	MXL
Peruvians in Lima, Peru	Peruvian	PEL
Puerto Ricans in Puerto Rico	Puerto Rican	PUR
East Asian ancestry (EAS)		
Chinese Dai in Xishuangbanna, China	Dai Chinese	CDX
Han Chinese in Beijing, China	Han Chinese	CHB
Southern Han Chinese	Southern Han Chinese	CHS
Japanese in Tokyo, Japan	Japanese	JPT
Kinh in Ho Chi Minh City, Vietnam	Kinh Vietnamese	KHV
European ancestry (EUR)		
Utah residents (CEPH) with Northern and Western European ancestry	CEPH	CEU
British in England and Scotland	British	GBR
Finnish in Finland	Finnish	FIN
Iberian Populations in Spain	Spanish	IBS
Toscani in Italia	Tuscan	TSI
South Asian ancestry (SAS)		
Bengali in Bangladesh	Bengali	BEB
Gujarati Indians in Houston, TX, USA	Gujarati	GIH
Indian Telugu in the UK	Telugu	ITU
Punjabi in Lahore, Pakistan	Punjabi	PJL
Sri Lankan Tamil in the UK	Tamil	STU

Supplementary Table 1 Subpopulation and population names with abbreviations.
All the names and abbreviations are the same as used by the 1000 Genomes Project.